JHEP PROCEEDINGS

Heavy Flavours 8, Southampton, UK, 1999

Spectroscopy of excited b and c states

V. Ciulli

European Laboratory for Particle Physics (CERN), 1211 Geneva 23, Switzerland
Email: Vitaliano.Ciulli@cern.ch

ABSTRACT: Recent results on the spectroscopy of excited b and c states are presented. In particular, these include the first observation of the D_1 (light quark spin $j = 1/2$) resonance, searches for radially excited $D^{*\prime}$ and observations of orbitally excited B^*_J states. The current experimental status on excited charmed baryons is also briefly reviewed.

The spectroscopy of hadrons containing a b or a c quark is greatly simplified by the fact that heavy-quark masses are much greater than the energy scale $\Lambda_{\rm QCD}$ of strong interactions. In the limit of infinite heavy-quark mass, heavy-light hadron physics can be described by an effective theory (HQET), which is invariant under changes of the flavour and spin of the heavy-quark [1, 2, 3]. The consequences of this heavy-quark symmetry (HQS) for spectroscopy have been worked out in [4]. The spin of the heavy quark and the total angular momentum j of the light degrees of freedom are separately conserved. Therefore hadronic states can be classified by the quantum numbers of the light quarks. Because of the spin symmetry, for fixed $j \neq 0$, there is a doublet of degenerate states with total spin $J = j \pm \frac{1}{2}$, and their total widths for a strong transition to an other doublet j' are the same. In addition the partial widths of the four possible transitions are also predicted by the symmetry. Finally, because of the flavour symmetry, all of the mass splittings and partial decay widths of these states are independent of the heavy-quark flavour.

Since the quark masses are not infinite, HQS is an approximate symmetry and corrections of order $\Lambda_{\rm QCD}/m_Q$ turn out to be important. HQET provides a framework for treating these corrections, which break the degeneracy of the levels. Therefore spectroscopic data are of invaluable importance to test the predictions of heavy-quark effective theory.

1. D mesons spectroscopy

The expected spectroscopy for D mesons is summarized in figure 1.

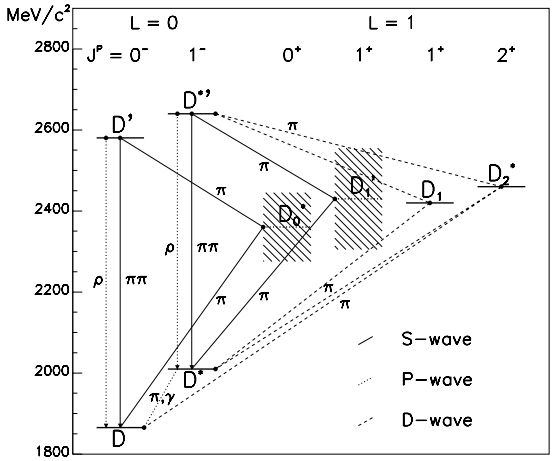

Figure 1: Spectroscopy of D mesons.

The D and D^* mesons, in which the light quark has orbital angular momentum $L = 0$, are well established and their properties and decays have been extensively studied [5].

Excited c mesons with orbital angular momentum $L = 1$, collectively called D^*_J, are classified into two spin doublets with light-quark angular momentum $j = \frac{1}{2}$ and $j = \frac{3}{2}$. According to HQS, the latter can only decay to $L = 0$ states through a D-wave and they are therefore expected to be narrow. The $j = \frac{1}{2}$ are instead expected to be wide resonances since they can decay via a S-wave. The observed $D_1(2420)$ and

$D_2^*(2460)$ are interpreted as the spin doublet $j = \frac{3}{2}$, with $J^P = 1^+$ and $J^P = 2^+$ respectively [5]. The first observation of the wide D_1^{*0} has been recently reported by CLEO II. It must be noted that a recent calculation [6, 7], which takes into account relativistic effects for the light quark, predict the mass difference between D_2^* and D_1^* to be negative (*spin-orbit inversion*). Therefore the observation of the $j = \frac{1}{2}$ doublet is important not only to confirm general HQS predictions, but also to give insight into this kind of effect.

A still controversial issue is the observation of the radial excitation $D^{*\prime}$ claimed by DELPHI, for similar analyses from OPAL and CLEO found no evidence.

In the strange sector of charmed mesons, in addition to the $L = 0$ states, $D_s^{\pm}$ and $D_s^{*\pm}$, two narrow resonances, the $D_{s1}^{\pm}(2536)$ and the $D_{sJ}^{\pm}(2573)$, compatible with the $L = 1\,(j = \frac{3}{2})$ doublet have been found [5], but no new data are available.

1.1 Observation of D_1^{*0} by the CLEO experiment

The first observation of the $D_1^{*0}(j = \frac{1}{2})$ meson has been recently reported by CLEO II [8, 9]. Using 3.1 fb^{-1} taken at the $\Upsilon(4S)$, they searched for the D_J^* in the decay $B^- \to D_J^{*0}\pi^-$, followed by $D_J^{*0} \to D^{*+}\pi^-$ and $D^{*+} \to D^0\pi^+$. By measuring the momenta of the three pions and using four-momentum conservation, the momenta of all particles can be constrained without any attempt to reconstruct the D^0 decay. This greatly enhances the statistical resolution, although it also increases the overall level of background.

As shown in figure 1, three of the D_J^* can decay to $D^*\pi$. The D_2^* and the D_1 through D-wave, and the D_1^* through S-wave. Since both the B and the π are pseudoscalar, the D_J^* is totally polarised and the relative contributions can be determined from a partial wave analysis of its decay. A four-dimension fit is performed to the helicities and the relative azimuth in $D_J^{*0} \to D^{*+}\pi^-$ and $D^{*+} \to D^0\pi^+$ decays, and the $D^*\pi$ invariant mass (shown in figure 2). In the fit, the two $J^P = 1^+$ states are allowed to mix, having angular contributions for both S-wave and D-wave decay, with a strong interaction phase

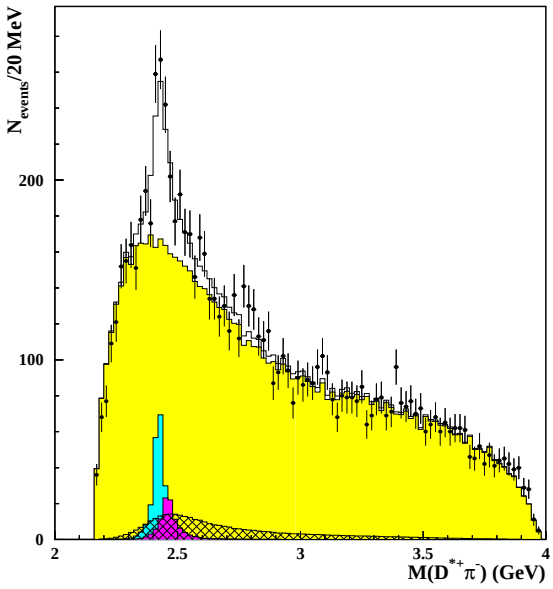

Figure 2: Mass spectrum of D_J^* candidates. The fitted resonances (two narrow and one wide) are shown.

difference in this interference term. The fit yields

$$m_{D_1^{*0}} = (2461^{+41}_{-34} \pm 10 \pm 32)\ \text{MeV}\ ,$$
$$\Gamma_{D_1^{*0}} = (290^{+101}_{-79} \pm 26 \pm 36)\ \text{MeV}\ .$$

where the first and second errors are respectively statistical and systematic, while the third one is due to the different chosen parametrisation of the strong phases. The fit favours $J^P = 1^+$ by 2σ with respect to the closest alternative (0^-).

In table 1 the measured D_1^{*0} mass is compared with the theory. The result is in agreement with HQS theory, but does not yet allow discrimination between different models (even if [7] seems to be disfavoured).

1.2 Searches for the radial excitation $D^{*\prime}$

Two charm radial excitations, a pseudoscalar and a vector state, respectively called D' and $D^{*\prime}$, are expected to exist with masses $m_{D'} \approx 2.58$ GeV/c^2 and $m_{D^{*\prime}} \approx 2.63$ GeV/c^2. The $D^{*\prime}$ is expected to decay in $D^*\pi\pi$, while the D' decays in $D\pi\pi$, with estimated decay widths of the order of a few MeV/c^2.

Evidence of the decay $D^{*\prime+} \to D^{*+}\pi^+\pi^-$ has been reported by DELPHI [11]. The D^{*+} is reconstructed in the decay mode $D^{*+} \to D^0\pi^+$, with either $D^0 \to K^-\pi^+$ or $D^0 \to K^-\pi^+\pi^+\pi^-$.

	$m_{D_1^{*0}}$(MeV)	$m_{D_1^0}$(MeV)	Δm(MeV)
measured	2461 ± 53	2422.2 ± 1.8[5]	$+39^{+42}_{-35}$
[10]	2460	2470	-10
[6]	2501	2414	$+87$
[7]	2585	2415	$+170$

Table 1: Comparison of CLEO preliminary result on D_1^{*0} mass with theoretical predictions.

A narrow peak is observed in the $D^{*+}\pi^+\pi^-$ invariant mass distribution, as shown in figure 3, whose width is compatible with the detector resolution. A signal of 66 ± 14 events, corresponding to 4.7σ significance, is obtained with an observed mass of $2637 \pm 2 \pm 6$ MeV/c^2 and upper limit of 15 MeV/c^2 at 95% C.L. on the full decay width. The corresponding production rate, relative to the orbitally excited D_1^0 and D_2^{*0} decaying to $D^{*+}\pi^-$, is

$$R = \frac{n(D^{*\prime +} \to D^{*+}\pi^+\pi^-)}{n(D_1^0, D_2^{*0} \to D^{*+}\pi^-)} = 0.49 \pm 0.21 \ .$$

The production rate is about the same in $c\bar{c}$ and $b\bar{b}$ events.

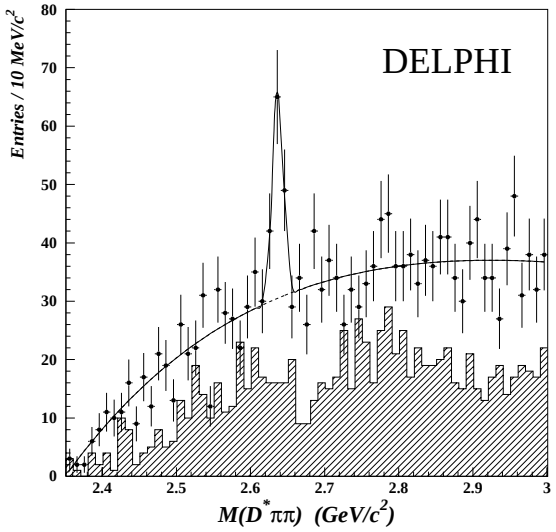

Figure 3: The $D^{*\prime}$ signal found by DELPHI (points). The hatched histogram shows the $D^{*+}\pi^-\pi^-$ combinations.

Searches for the decay $D^{*\prime +} \to D^{*+}\pi^+\pi^-$ have been performed by OPAL [12] and CLEO [9] too. OPAL use only $D^0 \to K^-\pi^+$ but claims a sensitivity similar to DELPHI. No evidence for a narrow resonance is found, yielding a limit $R < 0.21$ (95% C.L.). Figure 4 shows the $D^{*+}\pi^+\pi^-$ invariant mass distribution in data and in Monte Carlo, with the expected signal assuming DELPHI result. No signal was found by CLEO either, who used $D^0 \to K^-\pi^+\pi^0$ in addition to the decay modes used by DELPHI. The $D^{*+}\pi^+\pi^-$ invariant mass is shown in figure 5. Again no evidence for a signal is found and the limit set on the production relative to orbitally excited mesons is $R < 0.10$ (95% C.L.).

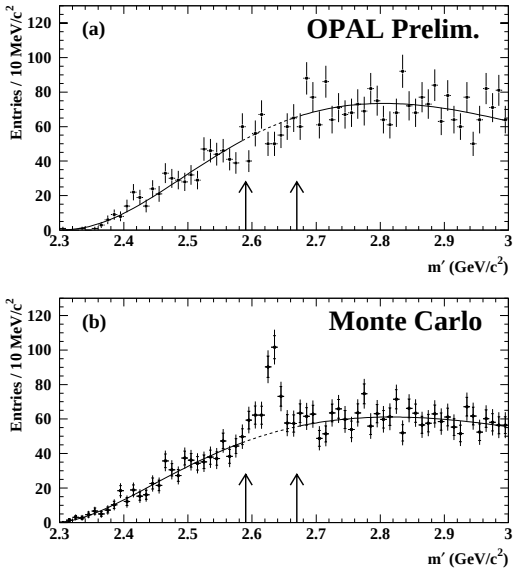

Figure 4: OPAL invariant mass distribution of $D^{*+}\pi^-\pi^+$ combinations in the data (top) and in the simulation (bottom). The $D^{*\prime}$ production rate in the simulated sample is fixed to the value measured by DELPHI.

2. B mesons spectroscopy

The spectroscopy of B mesons is expected to be very similar to that of D mesons, but up to now much less information is available compared with the charm sector.

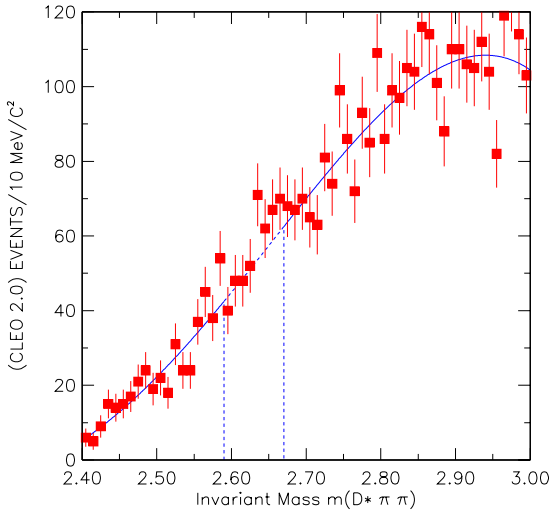

Figure 5: Mass of CLEO $D^{*\prime +}$ candidates.

The first experimental results on b excited states came from LEP, where the B mesons are produced in the decays $Z \to b\bar{b}$. Flavour-charge correlations and a resonant structure have been observed between the B mesons and nearby pions around an invariant mass of 5697 ± 9 MeV [5], being consistent with orbitally excited B_J^* mesons decaying to $B^{(*)}\pi$. Recently the CDF experiment at the Tevatron $p\bar{p}$ collider also reported a preliminary result on flavour-charge correlations consistent with the same hypothesis.

All these analyses are based on inclusive or partial reconstruction of B mesons, therefore the $B\pi$ mass resolution is only of order of 40 MeV. This does not allow identification of the B_2^* and B_1 narrow resonances separately, since they are expected to differ only by about 10 MeV. In addition, for decays to $B^*\pi$ where the photon in the subsequent decay $B^* \to B\gamma$ is not detected, the reconstructed B_J^* mass is shifted by -46 MeV$/c^2$. However several experiments attempted to investigate the structure and decays of these resonances by using different analysis approaches and trying to fit the mass spectrum under several model assumptions.

As far as bottom-strange mesons are concerned, no new results are available on the $B_{sJ}^*(5850)$ resonance [5], which is interpreted as coming from orbitally excited B_s mesons.

2.1 Observation of orbitally excited B at CDF

To search for B_J^*, CDF [13] uses B mesons partially reconstructed in semileptonic decays $B \to \ell\nu D^{(*)}$. This is a natural choice since the lepton provides an easy trigger for the event. The $D^{(*)}$ meson is fully reconstructed in several decay modes. Both the production and decay vertices of the B are reconstructed and used to estimate its flight direction, while its momentum is taken from the decay products, after rescaling by 15% for the neutrino. This partial reconstruction also allows the identification of the charge and flavour of the B meson.

Once a B is found, it is combined with all pions from the primary vertex to form B_J^* candidates. No selection is applied to the pions in order not to bias the invariant mass distribution. The analysis is performed in the variable $Q = m(B\pi) - m(B) - m(\pi)$, where the uncertainty on the B mass partially cancels out, and a 50 MeV resolution is achieved.

After the selection an excess in π charge — B flavour right-sign correlations is observed. In order to extract the signal several background sources have to be considered. These can be divided into *correlated* and *uncorrelated* backgrounds, depending on whether they are produced in association with the b quark (and therefore carry information on its charge and momentum) or whether they are independent of the presence of a heavy quark in the event. The latter are due to fake B candidates, "pile-up" events and particles from the "underlying" event and are subtracted from the sidebands in the selection cuts. The Q distribution after the subtraction of uncorrelated backgrounds is shown in figure 6. The remaining correlated background requires a more involved treatment, in particular that coming from hadronization tracks around the B meson. Pions produced in association with the b most probably give right-sign combinations. This is taken into account using a Monte Carlo inspired parametrization, which is fitted to the data together with the signal. Other correlated backgrounds are due to a few processes involving B mesons, which can be misidentified as B_J^* decays. The fit to the signal yields $\mathcal{B}(b \to B_J^*) = 0.28 \pm 0.06 \pm 0.03$, and as-

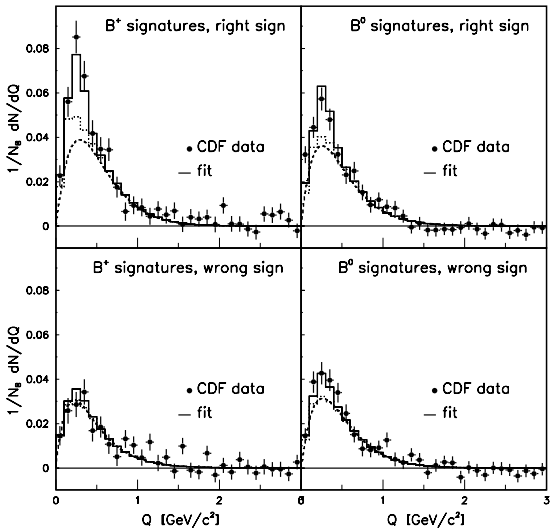

Figure 6: The sideband subtracted $B\pi^{\pm}$ Q distributions of the data (points) compared to the fit results. The dashed curves are the fitted hadronization component, the dotted histograms include all backgrounds, and the solid histograms are the totals including the B_J^* signal.

suming the mass splittings between the four B_J^* as in [7] the mass of the $B_1(J^P = 1^-,\ j = \frac{3}{2})$ is

$$m_{B_1} = 5.71 \pm 0.02\,\mathrm{GeV}/c^2\ .$$

2.2 ALEPH exclusive reconstruction of B_J^* states

A different, exclusive approach has been used by ALEPH in [14], where charged and neutral B mesons are fully reconstructed and used to study the $B\pi$ resonant structure. This exclusive approach clearly has the disadvantage of being statistically limited, but the $B\pi$ mass resolution is improved by one order of magnitude compared with inclusive analyses, and therefore it may allow the observation of a narrower structure. Furthermore, the identity and decay proper time of the B mesons are accurately known and there is a clear separation between tracks from the B decays and tracks from fragmentation. Therefore, using this method, one can study the possibility of tagging the flavour of the B neutral system at production by the charge of the nearby pion, which has important implications for the study of CP violation and mixing [15]. This tagging capability is clearly enhanced by the existence of resonant structure in the $B^{(*)}\pi$ system.

The B mesons are reconstructed in the decay modes $B \to D^{(*)}X$, where X is a $\pi^{\pm}$, a $\rho^{\pm}$ or an $a_1^{\pm}$, and $B \to J/\psi(\psi')X$, where X is a $K^{\pm}$ or a K^{*0}. The selection yields 238 B^+ and 166 B^0, 80% of the sample being in $B \to D^{(*)}X$ decay mode and the remaining 20% being in $B \to J/\psi(\psi')X$. Once a B meson is reconstructed, nearby pions are classified as "right-sign" or "wrong-sign" according to their charge. The right-sign track which has the highest momentum along the B direction and, in addition, gives an invariant mass with the B of less than 7.3 GeV/c^2 is selected to form a B_J^* candidate. Choosing instead the wrong-sign combination serves as a check on the estimate of the background and the reliability of the simulation. The B mass is constrained to its nominal value, yielding a $B\pi$ invariant mass resolution from 2 to 5 MeV/c^2 in the mass range from 5.5 to 5.8 GeV/c^2. The

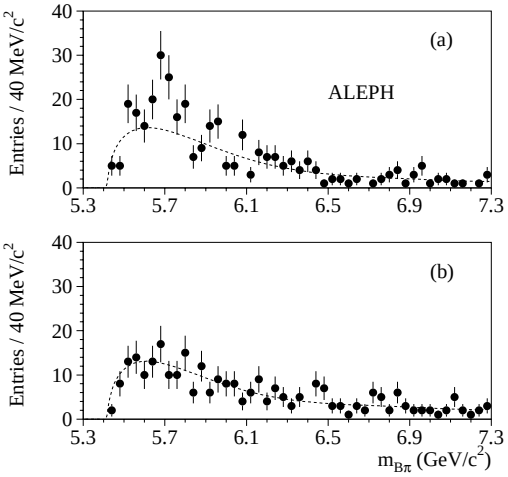

Figure 7: The $B\pi$ mass distribution in the ALEPH data with the expected background shapes for (a) right-sign and (b) wrong-sign candidates.

invariant mass distribution of the selected sample is shown in figure 7 for both right-sign and wrong-sign combinations. A fit to the signal with a single Gaussian yields a mass $m_{B_J^*} = 5695^{+17}_{-19}$ MeV/c^2, a width $\sigma = 53^{+26}_{-19}$ MeV/c^2 and a total of 43^{+17}_{-14} events. After correcting for the efficiency to reconstruct the pion and including the unobserved $B^{(*)}\pi^0$ decays, the production rate is

found to be

$$\frac{\mathcal{B}(b \to B_J^*)}{\mathcal{B}(b \to B_{u,d})} = (30^{+12}_{-10} \pm 3)\% \ .$$

These results on mass, width and production rate are in agreement with the results from inclusive analyses.

In the HQS framework, the B_J^* signal is the sum of the four different $L = 1$ states. The limited statistics do not permit detailed measurements of all parameters. Nevertheless assuming mass splittings and decay branching ratios as provided by the theory, the mass of the narrow doublet (here parametrized by the B_2^* mass) and the overall production rate of the four states can be fitted to the data. Table 2 shows the parameters used in the fit. The B_2^*, B_1 mass difference and widths, and the equality of the B_2^* branching ratios to $B^*\pi$ and $B\pi$, are as calculated in [16]. The masses and widths of the two wide states correspond to rough theoretical expectations [17]. The relative production rates are set according to spin counting. Finally the $B\pi$ mass spectra for the $B_J^* \to B^*\pi$ decays are displaced downward by 46 MeV/c^2 to take into account the missing soft photon from the $B^* \to B\gamma$ decay. Figure 8 shows a comparison of the mass

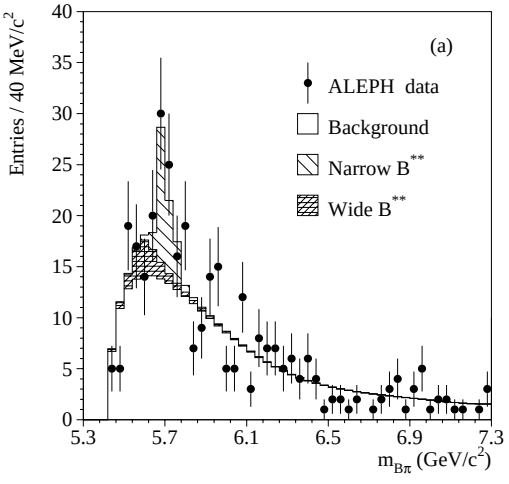

Figure 8: ALEPH right-sign $B\pi$ mass distribution from data with the results of the fit.

spectrum obtained from the fit and the data. The final values are

$$m_{B_2^*} = 5739^{+8}_{-11}(\text{stat})^{+6}_{-4}(\text{syst})\,\text{MeV}/c^2$$
$$\frac{\mathcal{B}(b \to B_J^*)}{\mathcal{B}(b \to B_{u,d})} = (31 \pm 9(\text{stat})^{+6}_{-5}(\text{syst}))\% \ .$$

The systematic error on the B_2^* mass is dominated by the uncertainty on the relative production rate, which is estimated by changing from spin to state counting, while the effect of varying the mass difference between B_2^* and B_1^* from 50 to 150 MeV/c^2 is only ± 1 MeV/c^2.

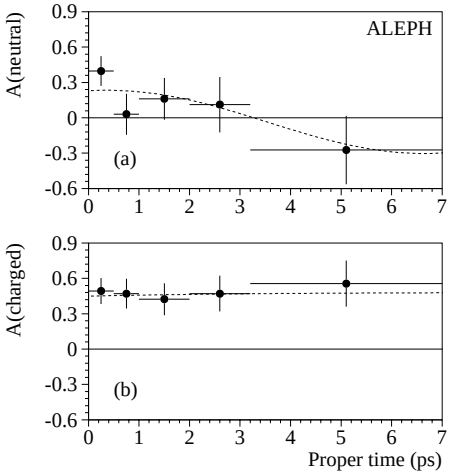

Figure 9: The right-sign/wrong-sign asymmetry $\mathcal{A}$ in the data as a function of the B proper decay time for (a) neutral and (b) charged B mesons. The dashed curves display the results of the fit.

The same $B\pi$ sample has been used to study the B flavour tagging based on the pion charge. Figure 9 shows the asymmetry $\mathcal{A} = (N_{rs} - N_{ws})/(N_{rs} + N_{ws})$ as a function of the B decay proper time, for both neutral and charged B mesons. The physical quantity of interest is the mistag rate ω_{tag}^N for neutral B's. This is extracted from $\mathcal{A}^N$ taking into account the effect of $B^0 - \bar{B}^0$ mixing. As a check the mistag rate has also been measured for charged B's, where $\mathcal{A}^C = (1 - 2\omega_{tag}^C)$, apart for a small dependence on proper time due to the different lifetime of the fake B's. The fit yields $\omega_{tag}^N = (34.4 \pm 5.5 \pm 1.0)\%$ and $\omega_{tag}^C = (26.0 \pm 3.6 \pm 0.7)\%$. On a high statistics sample of simulated events the mistag rate for neutral and charged B's are found to be, respec-

State	Mass (MeV/c^2)	Γ (MeV/c^2)	relative prod. rate	$\mathcal{B}(B\pi)$	$\mathcal{B}(B^*\pi)$
B_2^*	$m_{B_2^*}$	25	5/12	0.5	0.5
B_1	$m_{B_2^*} - 12$	21	3/12	–	1.0
B_1^*	$m_{B_2^*} - 100$	150	3/12	–	1.0
B_0^*	$m_{B_1^*} - 12$	150	1/12	1.0	–

Table 2: Properties, relative production rates and branching ratios as used by ALEPH in the fit to the $B\pi$ invariant mass spectrum.

tively, 36% and 32%, in good agreement with the above results. Further studies have shown that the difference in the mistag rates between neutral and charged B mesons is due to strange quark production in fragmentation. This spoils the isospin symmetry between the u and d quarks [18], since a $K^{\mp}$ is produced in association with a $B^{\pm}$, carrying flavour information, while a $\bar{K}^0(K^0)$ results in the fragmentation to a $B^0(\bar{B}^0)$. Unless there is perfect pion-kaon separation the mistag rate is therefore different, and charged B's cannot be used to infer results for the neutral B's.

2.3 L3 results on B_J^* spectroscopy

Preliminary results on the spectroscopy of excited B mesons have also recently been presented by L3 [19]. The mass and width of B_J^* have been measured using 1.25 million hadronic Z decays, where B meson candidates are inclusively reconstructed and combined with charged pions produced at the primary vertex.

The B direction is measured using combined information from the secondary vertex and track rapidity and the B energy is estimated from a kinematic constrained fit to the centre-of-mass energy. The obtained resolution on the $B\pi$ mass varies from 20 MeV/c^2 to 60 MeV/c^2, for energies between 5.6 GeV/c^2 and 5.8 GeV/c^2.

An excess of events above the expected background, estimated from the simulation, is found in the region $5.6 - 5.8$ GeV/c^2 (see figure 10). The signal has been fitted assuming a hyperfine splitting $m_{B_2^*} - m_{B_1} = m_{B_1^*} - m_{B_0^*} = 12\,\mathrm{MeV}/c^2$, but allowing both the mass of the B_2^* and of the B_1^* to vary freely. The widths $\Gamma_{B_2^*}$ and $\Gamma_{B_1^*}$ are also fitted, with the constraint $\Gamma_{B_1} = \Gamma_{B_2^*}$ and $\Gamma_{B_0^*} = \Gamma_{B_1^*}$, while the relative production rates are fixed to spin counting. The results of the fit are

$$\begin{aligned} m_{B_1^*} &= (5682 \pm 23)\,\mathrm{MeV}/c^2 \\ \Gamma_{B_1^*} &= (73 \pm 44)\,\mathrm{MeV}/c^2 \\ m_{B_2^*} &= (5771 \pm 7)\% \\ \Gamma_{B_2^*} &= (41 \pm 43)\,\mathrm{MeV}/c^2 \end{aligned}$$

with a χ^2 of 81 for 73 degrees of freedom. The fit is not a good description of the data in the region $5.9 - 6.0$ GeV/c^2 where an excess of data events over the simulated background is present. To take into account this excess, a high mass state, which can be interpreted as a radially excited B', has been included in the fit. The final results are

$$\begin{aligned} m_{B_1^*} &= (5670 \pm 10 \pm 13)\,\mathrm{MeV}/c^2 \\ \Gamma_{B_1^*} &= (70 \pm 21 \pm 25)\,\mathrm{MeV}/c^2 \\ m_{B_2^*} &= (5768 \pm 5 \pm 6)\% \\ \Gamma_{B_2^*} &= (24 \pm 19 \pm 24)\,\mathrm{MeV}/c^2 \end{aligned}$$

with a total of 2784 ± 274 events, corresponding to the branching ratio $\mathcal{B}(b \to B_J^* \to B^{(*)}\pi) = 0.32 \pm 0.03$. In addition 297 ± 100 events occupy the high-mass Gaussian, with $m_{B'} = 5936 \pm 22$ MeV/c^2 and $\sigma_{B'} = 50 \pm 23$ MeV/c^2. Figure 10 shows the results of the fit, for which the χ^2 is 63 for 67 degrees of freedom. The differences with respect to the results of the previous fit have been included in the systematic errors.

The above results place the average mass of the $j = 3/2$ states 98 ± 11 MeV/c^2 higher than that of the $j = 1/2$ states. This supports an earlier theoretical prediction [17] and disfavours the latest calculations [6, 7], which predicts spin-orbit inversion. To test the ability to discriminate between the two possible cases, additional fits have been performed, where the mass of the $j = 1/2$ states is constrained to be equal to or 100 MeV/c^2 higher than the mass of the $j = 3/2$

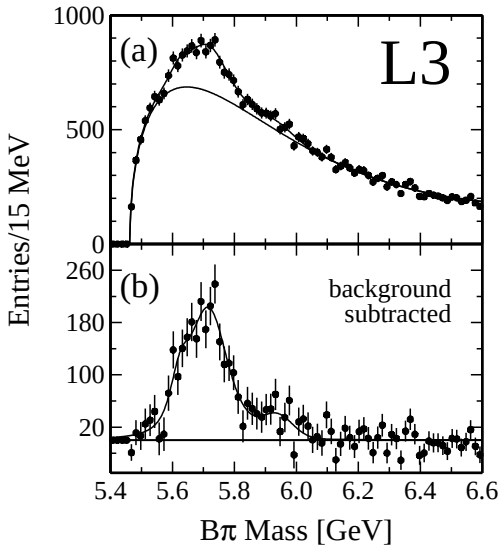

Figure 10: (a) Fit to the data $B\pi$ mass distribution. (b) The resulting background-subtracted distribution.

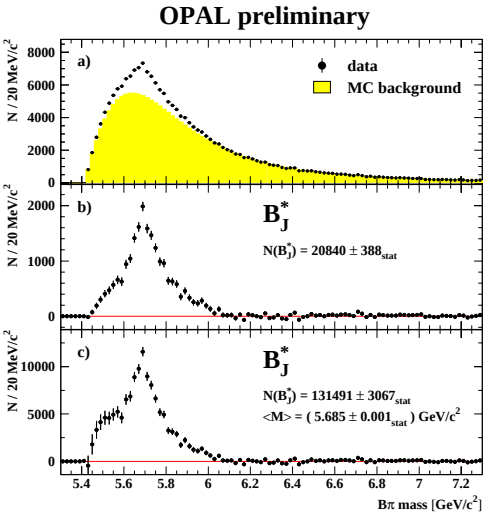

Figure 11: (a) The $B\pi$ mass distribution for data. (b) The Monte Carlo background-subtracted signal. (c) The efficiency-corrected B_J^* signal.

states. In both cases the fit likelihoods are lower than before, the highest one being 8.3% compared to 61.2% of the present fit.

2.4 OPAL study of the B_J^* decays

A preliminary result on $\mathcal{B}(B_J^* \to B^*\pi)$ has been recently presented by OPAL [20]. Using information of the photon in the decay $B^* \to B\gamma$, OPAL separates the $B_J^* \to B^*\pi$ decays from the $B_J^* \to B\pi$ ones and measures the $\mathcal{B}(B_J^* \to B^*\pi)$. This method gives insight into the decomposition of the B_J^* into the states allowed to decay to $B\pi$ (B_0^* and B_2^*) from the other states that can only decay to $B^*\pi$.

The analysis is based on an inclusive reconstruction of B_J^*, similar to the L3 one previously described. The mass spectrum of the $B\pi$ sample obtained is shown in figure 11. After a candidate B_J^* is found, photons and converted photons in the event are used to assess the probability of a $B^* \to B\gamma$ decay. The full sample is then divided into two subsamples, one enriched and the other depleted in B^*, and the $\mathcal{B}(B_J^* \to B^*\pi)$ is extracted from the number of candidates in the two subsamples. The result is

$$\mathcal{B}(B_J^* \to B^*\pi) = (85^{+26}_{-27} \pm 12)\% \,.$$

in agreement with theoretical predictions (see table 2).

The composition of the B_J^* sample is further investigated by extracting from the two subsamples the $B\pi$ mass distributions for the two decay modes, which are shown in figure 12. A significant excess of entries is seen in the pure $B_J^* \to B^*\pi$ distribution at masses around 5.7 GeV/c^2, with tails down to 5.5 GeV/c^2 and up to 6.0 GeV/c^2. The narrow peak is most likely due to B_1 and B_2^* decays, while the tails may be due to the wide B_1^* state. To obtain the true mass, the entries have to be shifted to higher mass by 46 MeV/c^2. In the pure $B_J^* \to B\pi$ mass distribution, a 2.2σ excess is observed at 5.8 GeV/c^2, as expected from B_2^* and B_0^* decays.

2.5 Summary on B_J^* states

A summary of present results on the spectroscopy of b excited states is shown in table 3, together with the predictions of several theoretical calculations. ALEPH and CDF results on B_2^* mass are in agreement between each other and with calculations in [6]. It must be noticed that they are both rather insensitive to the assumed mass splitting between the $j = 3/2$ and $j = 1/2$ doublets: changing the mass splitting from -160 MeV/c^2 to 100 MeV/c^2 results in an increase of the fitted

		$m_{B_2^*}(\mathrm{MeV}/c^2)$	$m_{B_1^*}(\mathrm{MeV}/c^2)$	$\Delta m(\mathrm{MeV}/c^2)$
measured	CDF[13]‡	$5725(5745) \pm 20$	–	$-160(100)^{\S}$
	ALEPH[14]	5739 ± 13	–	$100^{\S}$
	L3[19]‡	5768 ± 8	5670 ± 16	98 ± 24
predicted	[10]	5800	5780	20
	[6]	5733	5757	-24
	[7]	5715	5875	-160

Table 3: Comparison of experimental results and theoretical predictions on B_J^* masses. The results marked with a ‡ are still preliminary. The Δm, when marked with §, is fixed in the fit to the shown value.

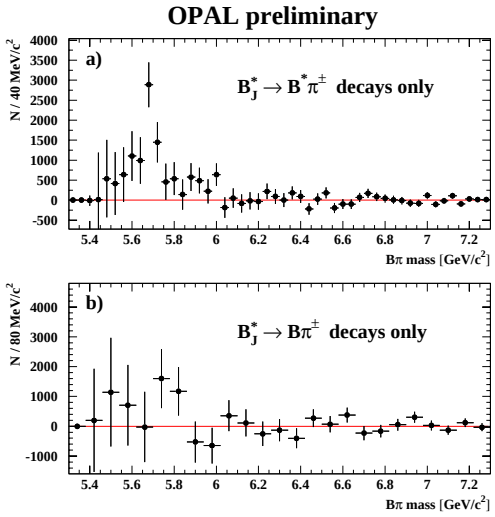

Figure 12: The $B\pi^\pm$ mass distribution of (a) $B_J^* \to B^*\pi^\pm$ and (b) $B_J^* \to B\pi^\pm$ transitions.

mass by 20 MeV/c^2 in CDF analysis, while the effect of a similar shift in the ALEPH result is only few MeV/c^2. The L3 result on the B_2^* mass is not in good agreement with ones discussed above, being higher by more than 2σ. This is the only analysis where the B_1^* mass is also measured and the result, if confirmed, would strongly disfavour models which predict large spin-orbit inversion [7].

3. Charmed baryon spectroscopy

As far as the charmed baryons are concerned, the most recent results concern evidence for the Ξ_c' and Ξ_{c1}, seen by CLEO [21, 22].

The Ξ_c' are csq baryons (where q can be either a u or a d quark) with the spin of the light quarks $S_{sq} = 1$ and $J^P = \frac{1}{2}^+$. Both charged and neutral Ξ_c' are observed to decay into $\Xi_c\gamma$.

Two new baryons decaying into $\Xi_c^{+*}\pi^-$ and $\Xi_c^{*0}\pi^-$ have been also observed by CLEO. These new states have been interpreted as the orbitally excited $J^P = \frac{3}{2}^-$ Ξ_{c1} baryons, since the $J^P = \frac{1}{2}^-$ Ξ_{c1}, would decay into $\Xi_c'\pi$.

A summary of the present experimental situation on charmed baryons is shown in figure 13. In the near future new results on charm baryon spectroscopy are also expected from the fixed target experiments FOCUS and SELEX.

4. Conclusions

We reviewed recent results on the spectroscopy of excited b and c states. All these results are in agreement with the expectations from Heavy Quark Symmetry. For the first time a wide $j = \frac{1}{2}$ state, namely the D_1^{*0}, has been observed. However, the observation of the radially excited $D^{*\prime}$ is still controversial. New studies of B_J^* resonances also support the existence of several states as predicted by HQS. In particular, if confirmed, both the measured D_1^{*0} mass and the fits to B_J^* masses, would disfavour models which predict large spin-orbit inversion.

References

[1] N. Isgur and M. B. Wise *Phys. Lett.* **B 232** (1989) 113; *Phys. Lett.* **B 237** (1990) 527.

[2] E. Eichten and B. Hill *Phys. Lett.* **B 234** (1990) 511.

[3] H. Georgi *Phys. Lett.* **B 240** (1990) 447.

[4] N. Isgur and M. B. Wise *Phys. Rev. Lett.* **66** (1991) 1130.

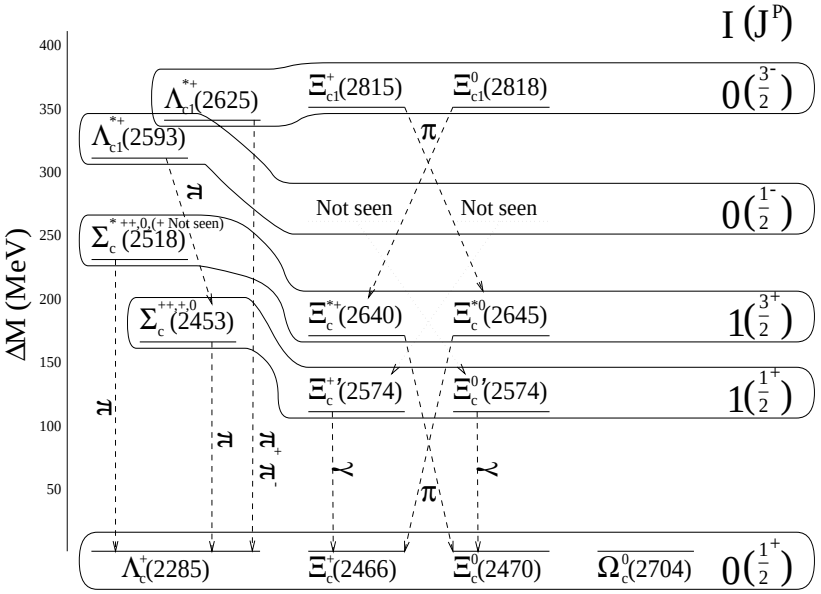

Figure 13: Spectroscopy of charmed baryons

[5] C. Caso *et. al.*, *Review of particle physics*, *Eur. Phys. J.* **C 3** (1998) 1 and 1999 off-year partial update for the 2000 edition available on the PDG WWW pages (URL:http://pdg.lbl.gov/).

[6] D. Ebert, V. O. Galkin, and R. N. Faustov *Phys. Rev.* **D 57** (1998) 5663, [hep-ph/9712318].

[7] N. Isgur *Phys. Rev.* **D 57** (1998) 4041.

[8] **CLEO** Collaboration, S. Anderson *et. al.*, *Observation of a broad $L = 1$ $c\bar{q}$ state in $B^- \to D^{*+}\pi^-\pi^-$ at CLEO*, [hep-ex/9908009].

[9] **CLEO** Collaboration, J. L. Rodriguez, *Hadronic decays of beauty and charm from CLEO*, [hep-ex/9901008].

[10] S. Godfrey and R. Kokoski *Phys. Rev.* **D 43** (1991) 1679.

[11] **DELPHI** Collaboration, P. Abreu *et. al. Phys. Lett.* **B 426** (1998) 231.

[12] **OPAL** Collaboration, *First evidence for a charm radial excitation, $D^{*\prime}$*, submitted to *XXIX International Conference on High Energy Physics, ICHEP 98 (Vancouver), July 23-28, 1998*, OPAL PN 352, July 14, 1998.

[13] **CDF** Collaboration, G. Bauer, *CDF B spectroscopy results: B^{**} and B_c^+*, [hep-ex/9909014].

[14] **ALEPH** Collaboration, R. Barate, *et. al. Phys. Lett.* **B 425** (1998) 215.

[15] J. Boudreau in *Proceedings of the 28th International Conference on High Energy Physics, Warsaw, Poland, July 25-31,1996* (Z. Ajduk and A.K.Wróblewski, eds.), p. 1224, World Scientific, 1997.

[16] E. J. Eichten, C. T. Hill, and C. Quigg *Phys. Rev. Lett.* **71** (1993) 4116, [hep-ph/9308337]. Updated in FERMILAB-CONF-94-118-T.

[17] M. Gronau and J. L. Rosner *Phys. Rev.* **D 49** (1994) 254, [hep-ph/9308371].

[18] I. Dunietz and J. L. Rosner *Phys. Rev.* **D 51** (1995) 2471, [hep-ph/9411213].

[19] **L3** Collaboration, *Measurement of the spectroscopy of orbitally excited B mesons at LEP*, submitted to *International Europhysics Conference High Energy Physics 99, Tampere, July 15-21,1999,* L3 Note 2423, June 15, 1999.

[20] **OPAL** Collaboration, *Investigation of the decay of orbitally-excited B mesons and first measurement of the branching ratio $BR(B_J^* \to B^*\pi)$*, submitted to *International Europhysics Conference High Energy Physics 99, Tampere, July 15-21, 1999,* OPAL PN400, July 7, 1999.

[21] **CLEO** Collaboration, C. P. Jessop *et. al. Phys. Rev. Lett.* **82** (1999) 492, [hep-ex/9810036] .

[22] **CLEO** Collaboration, J. P. Alexander *et. al.*, *Evidence of new states decaying into $\Xi_c^*\pi$*, [hep-ex/9906013].